Topology of an Amphiphilic Mitochondrial Signal Sequence in the Membrane-Inserted State: A Spin Labeling Study†

Yeon Gyu Yu, Thorgeir Elís Thorgeirsson, and Yeon-Kyun Shin*

Department of Chemistry, University of California, and Division of Structural Biology, Lawrence Berkeley Laboratory, Berkeley, California 94720

Received July 28, 1994; Revised Manuscript Received September 22, 1994®

ABSTRACT: To investigate the interaction of the presequence of the precursor of yeast cytochrome C oxidase subunit IV (COX IV) with phospholipid membranes, a series of single- and double-cysteine-substituted peptide variants derived from the 25-residue NH_2-terminal presequence has been synthesized and modified with nitroxide spin labels. The immersion depth, orientation, and secondary structure of the peptide in the POPC bilayer containing 10 mol % POPG were determined using electron paramagnetic resonance (EPR) spectroscopy. EPR saturation analysis of singly labeled variants reveals that the nitroxides attached to the NH_2-terminal region of the peptide insert into the acyl chain region of the bilayer, approximately 13 Å deep from the membrane surface. EPR line shape analysis of doubly labeled variants indicates that the peptide predominantly exists as an extended conformation, with little secondary structure. The experimental results, together with the energetic consideration of peptide−bilayer interactions, suggest that the presequence is located near the interface between the head group region and the acyl chain region, such that the hydrophobic side chains are solvated by the acyl chains and the charged side chains extended toward the polar environment at the bilayer surface.

Most mitochondrial proteins are encoded in nuclear genes and must be transported into the mitochondria after synthesis in the cytosol. Mitochondrial protein translocation requires NH_2-terminal targeting sequences, which are about 20−50-residue basic peptide segments that are cleaved off by proteases after transport into the appropriate compartments [for a review, see Dalbey and von Heijne (1992)]. Although they have high propensities to form amphiphilic α-helices composed of one hydrophobic face and another positively charged hydrophilic face (von Heijne, 1986), no distinct sequence homology has been found.

Questions concerning the nature of the recognition of the signal sequence by the mitochondrial membrane and the molecular details of protein translocation remain to be resolved. The presence of specific receptors in the outer membrane, such as MOM19 and MOM72 (Söllner et al., 1992), supports the idea of protein-mediated recognition of the targeting sequence. However, the fact that the signal sequences have the ability to bind to protein-free membranes, such as artificial lipid vesicles or protease-treated mitochondria (Roise, 1992), implies that the initial binding to the lipid bilayer might be a necessary step preceding interaction with translocators. On the other hand, it is possible that the signal sequence crosses the membrane without the aid of translocator proteins (Maduke & Roise, 1993). These questions regarding the significance of the membrane binding of presequences have led to a number of extensive spectroscopic studies aimed at investigating the topology and structure of membrane-bound presequences. Using circular dichroism (CD)[1] or NMR, the detailed secondary structures have been determined for some presequences in detergent micelles and in phospholipid vesicles (Roise et al., 1986; Endo et al., 1989; Karslake et al., 1990; Thornton et al., 1993). For most presequences, the depth of penetration and the orientation in the bilayer, which are perhaps essential for understanding the function of presequences, are yet to be determined (Wang et al., 1993).

Recently, techniques combining site-specific spin labeling and EPR analysis of spin-labeled polypeptides have emerged as powerful tools to investigate the structure and topology of membrane-bound peptides and proteins. This approach has been applied successfully to a variety of membrane proteins and membrane-interacting peptides or proteins, yielding information on the secondary structure, tertiary interactions, and immersion depth (Hubbell & Altenbach, 1994; Altenbach et al., 1990; Greenhalgh et al., 1991; Shin et al., 1993).

The presequence of cytochrome C oxidase subunit IV (COX IV) is a good model system to investigate bilayer−presequence interactions, since it is one of the best characterized presquences, both biochemically and genetically. A synthetic peptide representing the COX IV targeting sequence binds to mitochondria and artificial membrane systems (Roise et al., 1986; Tamm, 1991), competes with protein transport (Ito et al., 1985; Gillespie et al., 1985), and even translocates into lipid vesicles in the presence of transmembrane poten-

† Supported by the startup fund from the University of California at Berkeley, Lawrence Berkeley Laboratory LDRD Grant 3668-19, ACS PRF 28160-G7, and NIH Grant GM51290-01.

* Author to whom correspondence should be addressed.

® Abstract published in *Advance ACS Abstracts,* November 1, 1994.

[1] Abbreviations: CD, circular dichroism; COX IV, cytochrome C oxidase subunit IV; EDDA, ethylenediamine-*N,N'*-diacetic acid; EPR, electron paramagnetic resonance; HPLC, high-performance liquid chromatography; MOPS, 3-morpholinopropanesulfonic acid; MTSSL, *S*-(1-oxy-2,2,5,5-tetramethylpyrrolinyl-3-methyl)methanethiosulfonate spin label; NMR, nuclear magnetic resonance; PC, phosphatidylcholine; POPC, 1-palmitoyl-2-oleoylphosphatidylcholine; POPG, 1-palmitoyl-2-oleoylphosphatidylglycerol; T_1, spin−lattice relaxation time; T_2, spin−spin relaxation time.

0006-2960/94/0433-14221$04.50/0

tials (Maduke & Roise, 1993). Helical conformations of the peptide have been detected in membrane-like environments such as in detergent micelles and sonicated liposomes by CD (Roise et al., 1986) and NMR (Endo et al., 1989).

In this work, we report the secondary structure, orientation, and immersion depth of the signal sequence of COX IV determined with EPR analysis of spin-labeled peptides. We find that when the presequence binds to the membrane, (i) the spin labels insert deeply into the hydrocarbon chain region of the bilayer beneath the head group region; (ii) the peptide exists predominantly in an extended or random coil configuration; and (iii) the peptide is oriented parallel to the membrane surface.

MATERIALS AND METHODS

Materials. 1-Palmitoyl-2-oleoylphosphatidylcholine (POPC), 1-palmitoyl-2-oleoylphosphatidylglycerol (POPG), and 1-palmitoyl-2-steroyl-(*n*-doxyl)phosphatidylcholines (*n* = 5, 7) were obtained from Avanti Polar Lipids. *S*-(1-Oxy-2,2,5,5-tetramethylpyrrolinyl-3-methyl)methanethiosulfonate spin label (MTSSL) was obtained from Reanal (Hungary). Ni EDDA was a gift from Prof. W. L. Hubbell of the Jules Stein Eye Institute at the UCLA School of Medicine.

Peptide Synthesis. The peptide corresponding to the 25 NH_2-terminal residues of the COX IV precursor and the cysteine-substituted variants were synthesized by solid-phase peptide synthesis using (9-fluorenylmethoxy)carbonyl (Fmoc) amino acids (Fields & Noble, 1990) and a Wang Resin (Wang, 1973). Following synthesis, peptides were cleaved from the resin, and protecting groups were removed by treatment with a solution containing 85.5% trifluoroacetic acid, 5% water, 4.5% phenol, 2.5% anisol, and 2.5% dithioethanol for 5 h at room temperature (King et al., 1990). Then, the peptides were precipitated in *tert*-butyl methyl ether. A Vydac C_{18} reversed-phase HPLC column was used to purify the peptides using a 25−45% water/acetonitrile gradient containing 0.1% trifluoroacetic acid. The identity and purity of the peptides were confirmed by electrospray ionization mass spectrometry.

Spin Labeling. Cysteine-substituted variants were reacted with the thiol-specific MTSSL. The labeling reaction was performed in 10 mM MOPS buffer (pH 7.0) in the presence of a 5−10-fold molar excess of MTSSL, introduced by adding small amounts of a concentrated stock solution in acetonitrile. After 3−4 h of incubation at room temperature, the peptide was purified with HPLC. The single peak containing the spin-labeled peptide was isolated and lyophilized.

Vesicle Preparation. POPC and POPG were dissolved in chloroform and mixed to obtain the desired ratio of negatively charged lipid. The solvent was removed by a stream of nitrogen, and trace amounts of chloroform were removed by placing the lipid mixture under high vacuum for more than 1 h. The dry lipid was then resuspended in 20 mM MOPS buffer (pH 7.0), yielding a final lipid concentration of 65 mM. Vesicles were prepared by passing the mixture through 100 nm pore size polycarbonate membranes using a mini LiposoFast extruder (Avestine, Canada) after five cycles of freeze−thaw.

Electron Paramagnetic Resonance (EPR) Spectroscopy. EPR measurements were performed using a Bruker ESP300 EPR spectrometer (Bruker, Germany) equipped with a low-noise microwave amplifier (Mitech) and a loop-gap resonator (Medical Advances) capable of adapting gas-permeable TPX capillaries.

Power Saturation Experiments. Power saturation curves were obtained by measuring the peak-to-peak amplitude (I) of the first-derivative $M_I = 0$ EPR line as a function of the incident microwave power in the range 0.1−40 mW. The saturation curves were fitted to

$$I = A(P)^{1/2}/[1 + ((2)^{1/\epsilon} - 1)P/P_{1/2}]^{\epsilon} \quad (1)$$

with A, $P_{1/2}$, and ϵ as adjustable parameters. $P_{1/2}$ is the microwave power where the first-derivative amplitude is reduced to one-half of its unsaturated value. ϵ is a measure of the homogeneity of the saturation and varies from 1.5 to 0.5.

Collisions of nitroxides with relaxing reagents cause Heinsenberg spin exchange, effectively reducing the spin−lattice relaxation time T_1 and leading to an increase in the microwave power required to saturate the EPR lines. The quantity $\Delta P_{1/2}$ is the difference in $P_{1/2}$ values in the presence and absence of a relaxing reagent. $\Delta P_{1/2}$ is related to the Heisenberg exchange rate, W_{ex}, according to

$$\Delta P_{1/2} \propto W_{ex}/T_{2e}^{*} \quad (2)$$

where T_{2e}^{*} is the electron spin−spin relaxation time. Since W_{ex} is proportional to DC, where D is the relative diffusion coefficient and C is the concentration of the relaxing reagent, $\Delta P_{1/2}$ serves as a good estimate for the accessibility of the nitroxide to the relaxant, from which the local environment surrounding the nitroxide may be deduced. For example, in a membrane/water system, nonpolar molecules preferentially partition into the membrane phase, and the polar molecules prefer the aqueous phase. Thus, a nitroxide buried in the lipid bilayer experiences a high collision rate with nonpolar oxygen molecules, while the rate of collisions with water-soluble relaxants such as the Ni EDDA complex is much smaller. This approach has been very useful for determining the topology and the secondary structure of membrane-bound peptides and proteins.

Depth Measurements. Using spin-labeled mutants of bacteriorhodopsin, Hubbell and co-workers have recently developed a method to determine the immersion depth of the nitroxide from the membrane surface based on the ratio of $\Delta P_{1/2}$ values for membrane-soluble (O_2) and aqueous (M) relaxing reagents (Altenbach et al., 1994). It has been found that Φ, the natural log of the ratio of the $\Delta P_{1/2}$ value for the molecular oxygen ($\Delta P_{1/2}(O_2)$) to that for the metal ion complex ($\Delta P_{1/2}(M)$), is linearly proportional to the immersion depth d:

$$\Phi = \ln(\Delta P_{1/2}(O_2)/\Delta P_{1/2}(M)) = Sd + C \quad (3)$$

where S is the slope and C is the intercept. Experiments have also revealed that S is nearly the same for different metal ion complexes. In the present work, Ni EDDA complex was used as M. The depth calibration with bacteriorhodopsin for Ni EDDA has been supplied by the Hubbell group. As a control, we determined the depths of 5-doxyl-PC and 7-doxyl-PC in the phospholipid membrane (cf. Figure 5).

a

NH_2-M L S L R Q S I R F F K P A T R T L C S S R Y L L-COOH	PCOX
· · C · · · · · · · · · · · · · · · S · · · · · ·	PCOX3
· · · C · · · · · · · · · · · · · · S · · · · · ·	PCOX4
· · · · C · · · · · · · · · · · · · S · · · · · ·	PCOX5
· · · · · C · · · · · · · · · · · · S · · · · · ·	PCOX6
· · · · · · C · · · · · · · · · · · S · · · · · ·	PCOX7
· · · · · · · C · · · · · · · · · · S · · · · · ·	PCOX8
· · C C · · · · · · · · · · · · · · S · · · · · ·	PCOX34
· · C · · · C · · · · · · · · · · · S · · · · · ·	PCOX37

b

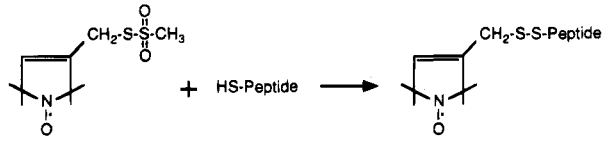

FIGURE 1: Amino acid sequences for the peptides used in this study. The first row shows the sequence of the peptide corresponding to the 25 N-terminal residues of cytochrome C oxidase IV precursor. In the subsequent rows, only substitutions are indicated with the appropriate letter codes for amino acids. (b) The spin-labeling reaction that couples the thiol-specific reagent *S*-(1-oxy-2,2,5,5-tetramethylpyrrolinyl-3-methyl) methanethiosulfonate (MTSSL) to the cysteine residue.

RESULTS

To investigate the topology of the NH_2-terminal region of the COX IV presequence in the membrane, we synthesized a wild-type peptide (PCOX) that contains a unique cysteine at position 19 and six single-cysteine-substituted variants, allowing site-specific nitroxide spin labeling (Figure 1). We also prepared two doubly labeled variants to study the secondary structure (Millhauser, 1992). For all variants, the single native cysteine at position 19 was replaced by serine.

The EPR spectrum of the spin-labeled PCOX in solution without lipid vesicles is shown in Figure 2a. This is a typical fast motion EPR spectrum for the nitroxide attached to a short peptide in solution. We obtained nearly identical spectra for all six singly labeled variants. Detailed information on the secondary structure of the peptide can be rather conveniently obtained from doubly labeled peptides. For two nitroxides in close proximity, the spin−spin interaction effectively broadens EPR lines allowing ranking spatial separations of the two nitroxides attached to several judiciously chosen pairs of sites in order, from which the secondary structure can be readily inferred. For example, an α-helix has 3.6 residues per turn, and thus residues three or four apart along the sequence [$(i, i + 3)$ or $(i, i + 4)$] are spatially much closer than residues one or two apart [$(i, i + 1)$ or $(i, i + 2)$]. Thus, the EPR spectra of $(i, i + 3)$ and $(i, i + 4)$ should be much broader than those of $(i, i + 1)$ and $(i, i + 2)$ for a well-defined α-helix. On the other hand, the spatial separation of $(i, i + 1)$ should be nearly the same as that of $(i, i + 4)$ for an extended conformation, yielding nearly identical spectra for $(i, i + 1)$ and $(i, i + 4)$ (Miick, 1993). For the two doubly labeled peptides (PCOX34 and PCOX37) in solution, we obtained nearly identical spectra (Figure 3a), indicating that the peptide is in an extended conformation. This is consistent with previous findings with CD that the secondary structure of the presequence in solution is not well-defined (Tamm, 1991) or it is predominantly random coil (Roise et al., 1986).

EPR spectra of spin-labeled variants in the presence of POPC vesicles containing 10 mol % POPG are shown in Figure 2b. In comparison with the fast motional solution spectrum in Figure 2a, spectral lines become much broader, indicating retarded motion of the nitroxide due to the interaction with the more viscous membrane phase. In fact, EPR line shapes are very similar to those typically found for the nitroxide attached to membrane-bound peptides

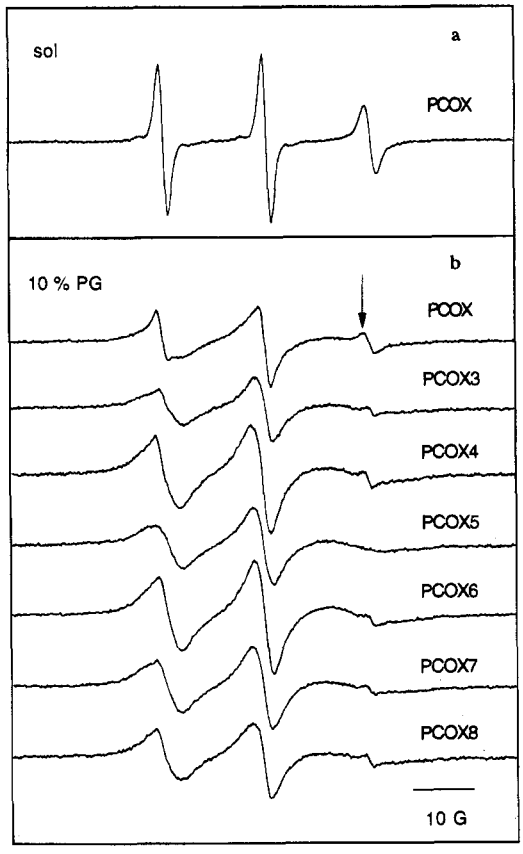

FIGURE 2: (a) First-derivative EPR spectrum for the spin-labeled PCOX peptide in 20 mM MOPS buffer (pH 7.2). (b) EPR spectra for spin-labeled peptides in the presence of POPC/POPG lipid vesicles (10 mol %) in 20 mM MOPS buffer (pH 7.2). The final peptide concentrations were 30−40 μM, and the phospholipid concentration was 50 mM (lipid-to-peptide ratio ≈ (1−2) × 10^3).

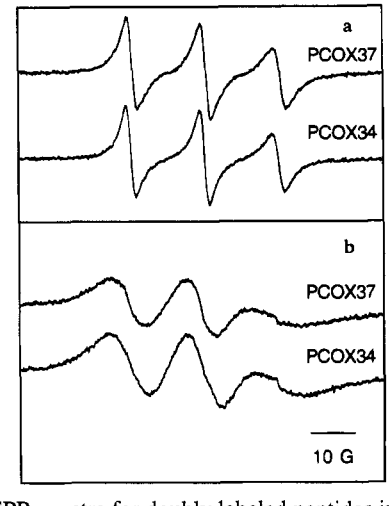

FIGURE 3: EPR spectra for doubly labeled peptides in solution and bound to POPC lipid vesicles containing 10 mol % POPG: (a) solution spectra for PCOX34 and PCOX37 in 20 mM MOPS buffer (pH 7.2); (b) spectra for PCOX34 and PCOX37 in vesicles. The final peptide concentrations were 30−40 μM, and the phospholipid concentration was 50 mM.

(Altenbach & Hubbell, 1988; Yu et al., 1994), and the estimated rotational correlation times are approximately in the range of 3−4 ns. These clearly indicate that the spin-labeled variants are mostly bound to the phospholipid bilayer. Most EPR spectra in Figure 2b contain a sharp spectral component, which is best seen in the high-field lines as indicated by an arrow. Considering that the presequence reversibly binds to membranes (Roise, 1992), this is most likely from the unbound peptide species in the aqueous phase. Under the present experimental conditions, the unbound fraction of the peptide estimated by spectral subtraction is 1−5%, depending on the spin-labeled position. Unreacted free spin label would give rise to the same sharp spectral component. Since the peptide and the free spin label are well resolved in reversed-phase HPLC, it is not likely that samples are contaminated with the free spin label.

The most noticeable feature of the EPR spectra for membrane-bound peptides is the reduced solvent-sensitive hyperfine coupling constant, A_N. The A_N values for all singly labeled peptides in solution are nearly the same, 16.1 ± 0.2 G, which is a typical A_N for the MTSSL spin label in water.[2] On the other hand, the A_N values are in the range 14.8−15.0 G when peptides are bound to vesicles, indicating that the nitroxides are in a nonpolar environment (Seelig & Hasselbach, 1971), most likely the hydrocarbon chain region of the bilayer. In fact, these A_N values are nearly the same as those found for the same nitroxide attached to the lipid-exposed residues on bacteriorhodopsin (Altenbach et al., 1990). The A_N value for PCOX, in which the nitroxide is near the COOH terminus, also corresponds to a nonpolar environment, suggesting that the entire peptide is inserted into the bilayer.

To obtain further detailed information on the depth and orientation of the presequence in the phospholipid bilayer, EPR saturation experiments were performed for all singly labeled variants under nitrogen, under air, and in the presence of Ni EDDA under nitrogen. Typical EPR saturation curves for a spin-labeled peptide bound to the lipid bilayer, under various conditions, are shown in Figure 4. The $\Delta P_{1/2}$ values for all spin-labeled variants bound to 10% charged vesicles are listed in Table 1. For all variants, high $\Delta P_{1/2}(O_2)$ values and low $\Delta P_{1/2}$(Ni EDDA) values were obtained, again indicating that the nitroxides attached to the peptides are located substantially deep in the bilayer. For comparison, the $\Delta P_{1/2}$ values for the spin-labeled (5-doxyl and 7-doxyl) phosphatidylcholine derivatives in both types of vesicles have been determined. The Φ values for these spin labels are similar to those obtained for the lipid-bound peptides, implying that the nitroxides attached to the peptides are embedded near the fifth and seventh carbons of the acyl chain in the bilayer.

The immersion depth of the nitroxide attached to each peptide was determined using eq 3 with $S = 0.286$ and $C = -2.62$, which represents the immersion depth calibration with spin-labeled bacteriorhodopsin mutants for 200 mM Ni EDDA. The depth profile is plotted against the spin-labeled position in Figure 5.

Two important features are apparent in the depth profile shown in Figure 5: (i) the nitroxides attached to the peptide insert into the hydrocarbon chain region of the bilayer and (ii) the NH_2-terminal region is parallel to the membrane surface. The average depth of the nitroxides is 13 Å from

[2] The hyperfine coupling constant was obtained by measuring the peak-to-peak distance.

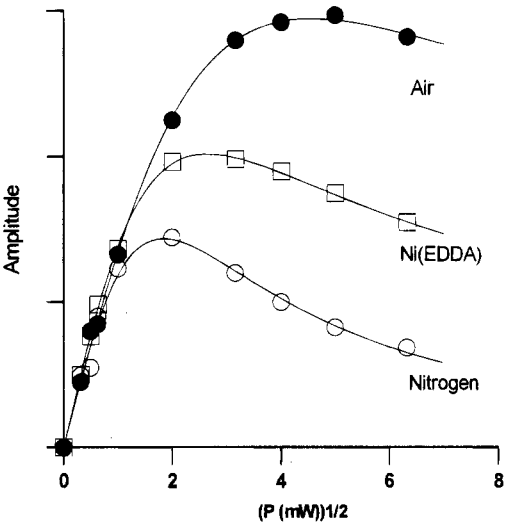

FIGURE 4: Power saturation curves for the PCOX4 peptide in POPC vesicles containing 10 mol % POPG. The data were obtained by measuring the peak-to-peak amplitude of the $M_I = 0$ line of the first-derivative EPR spectrum. Using a 5 μL sample placed in a gas-permeable plastic TPX capillary, the EPR spectra were collected at 0.1, 0.25, 0.4, 1.0, 4.0, 10, 16, 25, and 40 mW incident microwave powers under three different conditions: under nitrogen flow in the absence of paramagnetic reagents (○); under nitrogen in the presence of 10 mM Ni EDDA (□); and under the flow of air (●). The curves are the least-squares fits to eq 1 with $P_{1/2}$ values of 2.8 mW (N_2), 6.3 mW (Ni EDDA), and 18.1 mW (air).

Table 1: $\Delta P_{1/2}$ and Φ Values for Spin-Labeled Variants Bound to POPC Vesicles Containing 10 mol % POPG

	$\Delta P_{1/2}$(air)/$\Delta P_{1/2}$(Ni EDDA) (mW)	Φ
PCOX	(11.7 ± 1.0)/(6.2 ± 1.2)	0.7 ± 0.3
PCOX3	(13.8 ± 1.6)/(3.2 ± 2)	1.7 ± 0.8
PCOX4	(15.3 ± 1.3)/(3.5 ± 0.3)	1.5 ± 0.2
PCOX5	(14.0 ± 1.5)/(4.1 ± 1.2)	1.3 ± 0.4
PCOX6	(15.2 ± 0.4)/(5.3 ± 0.7)	1.1 ± 0.2
PCOX7	(17.3 ± 1.6)/(5.4 ± 1.5)	1.2 ± 0.3
PCOX8	(16.5 ± 1.6)/(3.8 ± 1.4)	1.5 ± 0.6
5-doxyl-PC	(9.6 ± 0.5)/(3.4 ± 1.5)	1.1 ± 0.5
7-doxyl-PC	(10.7 ± 0.6)/(1.8 ± 1.0)	2.0 ± 0.7

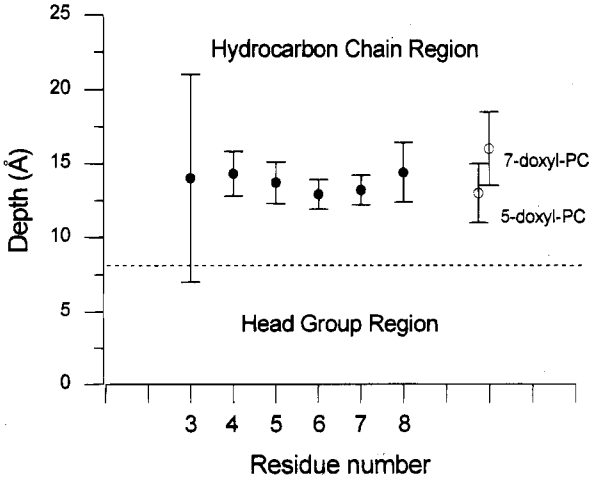

FIGURE 5: Plot of the immersion depth vs residue number. Also shown are the estimated depths of the spin probes of 1-palmitoyl-2-stearoyl-(*n*-doxyl)-PC ($n = 5$ and 7). In this analysis, the 5-doxyl-PC served as a standard, determining the intercept in eq 3. The concentration of Ni EDDA was 200 mM.

the surface, approximately 4−5 Å below the head group/hydrocarbon chain boundary. The depth profile is nearly parallel to the membrane surface although there is some variation. Little variation in depth through the six residues of the NH_2 terminus (3−8) and the similar depth for position 19 indicate that the whole peptide is perhaps oriented parallel to the surface of the membrane.

Information on the secondary structure of the peptide in the membrane-inserted state was deduced from doubly labeled peptides. In Figure 3b, EPR spectra of doubly labeled PCOX34 and PCOX37 in the presence of vesicles are shown. In comparison with the spectra of singly labeled peptides, there is significant line broadening due to spin−spin interactions between the two spatially close nitroxides. We also found that the spectrum of PCOX37 is somewhat broader than that of PCOX34, indicating that the two nitroxides on residues four apart are spatially closer than the two on residues one apart. This suggests that the peptide contains a slight α-helical character, although the difference in line broadening between $(i, i + 1)$ and $(i, i + 4)$ is much less than what would have been expected for a well-defined α-helix (Millhauser, 1992). We therefore conclude that the peptide is predominantly in an extended conformation.

DISCUSSION

In this work, it was found that the nitroxides attached to varius positions in the NH_2-terminal region of the peptide derived from the COX IV targeting sequence insert into the hydrocarbon chain region of the POPC bilayer containing 10 mol % POPG, approximately 13 Å deep from the membrane surface with little positional dependence (Figure 5). However, the depth of the nitroxide does not necessarily reflect the average immersion depth of the peptide backbone. Since the average distance from the α-carbon to the nitroxide group for the MTSSL spin label is estimated to be ~6 Å (Rabenstein & Shin, unpublished results), the backbone of the peptide chain can be either as shallow as 7 Å or as deep as 19 Å from the surface. A substantial polarity gradient exists in the bilayer. Thus, a strongly apolar side chain would preferentially orient toward the hydrophobic core rather than toward the surface.

The nitroxide side chain is fairly apolar, so that it may preferentially partition into the hydrophobic acyl chain region. In order to understand the effects of spin labeling, the hydrophobicity of the spin-labeled cysteine was estimated by examining the binding equilibria of PCOX34 and PCOX3 to POPC vesicles containing 4 mol % POPG. PCOX3 contains leucine at position 4, while PCOX34 contains a spin-labeled cysteine in replacement of leucine at that position. They are otherwise identical. The natural log of the ratio of the binding constants therefore gives the change in the free energy of transfer ($\Delta\Delta G$) corresponding to the substitution of leucine by spin-labeled cysteine. We found that $\Delta\Delta G = -0.7$ kcal/mol, indicating that spin-labeled cysteine is somewhat more apolar than leucine. In fact, this $\Delta\Delta G$ value put the spin-labeled cysteine somewhere between methionine and tryptophan on a hydrophobic scale (Engelman et al., 1986). The change in the hydrophobic energy caused by the introduction of spin-labeled cysteine is not sufficient to alter the backbone position of the entire peptide or to extensively perturb the conformation of the peptide. However, the nitroxide side chain likely has a tendency to orient preferentially toward the more hydrophobic acyl chain region, perhaps leading to some overestimation of the depth for polar residues. Thus, it is quite possible that the peptide backbone is located at a depth shallower than 13 Å, but deeper than 7 Å.

At room temperature, the peptide in the bilayer appears to be predominantly in an extended conformation. In the case of a well-defined α-helix, the spectrum of PCOX37 would have been much broader than that of PCOX34 (Figure 3b) (Millhauser, 1992), and the small variation in immersion depth throughout the six consecutive residues in the NH_2-terminal region is consistent with an equilibrium well shifted toward an extended conformation. [For a well-defined stationary α-helix, a depth variation of at least 10 Å in amplitude with a periodicity of 3.6 residues is expected.] However, it is also possible that the depth profile in Figure 5 is biased due to the apolar nature of the spin-labeled cysteine, and/or it is somewhat averaged due to thermal fluctuations, resulting less positional dependence than what would have been expected for the stationary state. On the other hand, little or no helical structure was detected with CD for the presequence in membranes containing less than 20% negatively charged lipid (Tamm & Bartholdus, 1990). Thus, considering the large free energy cost of buring an incompletely hydrogen-bonded peptide in the nonpolar environment (5.6 kcal/mol per hydrogen bond), it is most likely that the peptide backbone stays in a polar environment.

According to a simple treatment of the energetics of polypeptide insertion into membranes by Engelman and Steitz (1981), for the 25-residue peptide the lower limit of the hydrophobic free energy of transfer from water to the lipid phase would be on the order of −40 kcal/mol, but this favorable free energy on insertion will be offset by and large by a loss of conformational entropy. However, the energy cost of burying six positive charges and the negatively charged carboxyl end in the hydrophobic acyl chain region would be more than 100 kcal/mol, which far exceeds the free energy gain of hydrophobic origin. Thus, the charged groups are expected to stay in a polar environment.

Taking both the experimental results and energetic arguments together, the peptide backbone is likely located near the interface between the polar head group region, which is ~8 Å thick, and the acyl chain region, so that the hydrophobic side chains are solvated by the hydrophobic acyl chain region, with the charges on the lysines and arginines remaining in the polar environment.

The hydrophobic energy is perhaps the main driving force for insertion of the presequence into the bilayer. For an amphiphilic helix, the positive charges would align on the hydrophilic face. Thus, the electrostatic repulsion between the positive charges could act as a main opposing force preventing helix formation. For this presequence, it has been found that negatively charged lipid promotes helix formation (Tamm & Bartholus, 1990). With more negatively charged lipid, the repulsion between positively charged residues might be reduced due to increased electrostatic interactions between the positively charged residues and negative charges from the lipid, leading to the stabilization of the helix.

Such an interplay of electrostatic effects and hydrophobic interactions can also be seen in the membrane insertion of an amphiphatic peptide derived from CTP: phosphocholine cytidylyltransferase (PCT). Although no binding to un-

charged vesicles was observed, the presence of anionic lipid leads to insertion into the bilayer and enhanced helix formation (Johnson & Cornell, 1994). Furthermore, measurements of tryptophan fluorescence in the presence of lipid-bound quenchers revealed that a residue on the hydrophobic side of the helix was buried at a depth corresponding to the ninth carbon on the acyl chain of the lipid. The PCT peptide contains a number of positively charged residues, although it is negative overall, whose interactions with the negatively charged lipid head groups might stabilize the peptide in the membrane and promote helix formation in a manner similar to what has been proposed for the COX IV peptide.

Currently, it is not clear whether the mitochondrial presequences serve as recognizing motifs for translocation machinery (Pfanner & Neupert, 1987; Verner & Schatz, 1987) or actively lead protein translocation through the bilayer (von Heijne, 1986; Roise et al., 1986). Recently, it has been shown that the COX IV presequence can be imported through protein-free membranes in a transmembrane potential-dependent manner (Maduke & Roise, 1993). Thus, in mitochondria, direct transport not involving protein translocators is still a possibility. Alternatively, insertion of the presequence into the phospholipid bilayer as an initiation step for the translocation can at least lead to facilitated recognition by translocators through efficient two-dimensional diffusion inside mitochondrial membranes.

ACKNOWLEDGMENT

We thank Dr. D. S. King for mass spectrometry and Drs. W. L. Hubbell and C. Altenbach for sending us the bacteriorhodopsin depth calibration data.

REFERENCES

Altenbach, C., & Hubbell, W. L. (1988) *Proteins 3*, 230−242.

Altenbach, C., Marti, T., Khorana, H. G., & Hubbell, W. L. (1990) *Science 248*, 1088−1092.

Altenbach, C., Greenhalgh, D. A., Khorana, H. G., & Hubbell, W. L. (1994) *Proc. Natl. Acad. Sci. U.S.A. 91*, 1667−1671.

Dalbey, R. E., & von Heijne, G. (1992) *Trends Biochem. Sci. 17*, 474−478.

Endo, T., Shimada, I., Roise, D., & Inagaki, F. (1989) *J. Biochem. 106*, 396−400.

Engelman, D. M., & Steitz, T. A. (1981) *Cell 23*, 411−422.

Engelman, D. M., Steitz, T. A., & Goldman, T. (1986) *Annu. Rev. Biophys. Biophys. Chem. 15*, 321−353.

Field, G. B., & Noble, R. L. (1990) *Int. J. Pept. Protein Res. 35*, 161−214.

Gillespie, L. L., Argan, C., Taneja, A. T., Hodges, R. S., Freeman, K. B., & Shore, G. C. (1985) *J. Biol. Chem. 260*, 16045−16048.

Greenhalgh, D., Altenbach, C., Hubbell, W. L., & Khorana, H. G. (1991) *Proc. Natl. Acad. Sci. U.S.A. 88*, 8626−8630.

Hubbell, W. L., & Altenbach, C. (1994) Site-directed spin labeling of membrane proteins in *Membrane Protein Structure: Experimental Approaches* (White, S., Ed.) Oxford Press.

Ito, A., Ogishima, T., Ou, W., Omura, T., Aoyagi, H., Lee, S., Mihara, H., & Izumiya, N. (1985) *J. Biochem.* (Tokyo) *98*, 1571−1582.

Johnson, J. E., & Cornell, R. B. (1994) *Biochemistry 33*, 4327−4335.

Karslake, C.; Piotto, M. E., Pak, T., Weiner, H., & Gorenstein, D. G. (1990) *Biochemistry 29*, 9872−9878.

King, D., Fields, C., & Fields, G. (1990) *Int. J. Pept. Protein Res. 36*, 255−266.

Maduke, M., & Roise, D. (1993) *Science 260*, 364−367.

Miick, S. M. (1993) Ph.D. Thesis, University of California at Santa Cruz, Santa Cruz, CA.

Millhauser, G. L. (1992) *Trends Biochem. Sci. 17*, 448−452.

Pfanner, N., & Neupert, W. (1985) *J. Biol. Chem. 262*, 7528−7536.

Roise, D. (1992) *Proc. Natl. Acad. Sci. U.S.A. 89*, 608−612.

Roise, D., Horvath, S. J., Tomich, J. M., Richards, J. H., & Schatz, G. (1986) *EMBO J. 5*, 1327−1334.

Seelig, J., & Hasselbach, W. (1971) *Eur. J. Biochem. 21*, 17−21.

Shin, Y. K., Levinthal, F., Levinthal, C., & Hubbell, W. L. (1993) *Science 259*, 960−963.

Söllner, T., Rassow, J., Wiedmann, M., Schlossmann, J., Keil, P., Neupert, W., & Tamm, L. K. (1991) *Biochim. Biophys. Acta 1071*, 123−148.

Tamm, L. K., & Bartoldus, I. (1990) *FEBS Lett. 272*, 29−33.

Thornton, K., Wang, Y., Weiner, H., & Gorenstein, D. G. (1993) *J. Biol. Chem. 268*, 19906−19914.

Verner, K., & Schatz, G. (1987) *EMBO J. 6*, 2449−2456.

von Heijne, G. (1986) *EMBO J. 5*, 1335−1342.

Wang, S.-S. (1993) *J. Am. Chem. Soc. 95*, 1328−1333.

Wang, Z., Jones, J. D., Rizo, J., & Gierasch, L. M. (1993) *Biochemistry 32*, 13991−13999.

Yu, Y. G., King, D. S., & Shin, Y. K. (1994) *Science 266*, 274−276.